ISSN (Print) 1226-1750
ISSN (Online) 2233-6656
Journal of Magnetics 24(3), 512-517 (2019) https://doi.org/10.4283/JMAG.2019.24.3.512

Investigation of The Magnetic Properties of Zn_2TiO_4 Single Crystal

Ying Liu[1,2], Liang Li[1], Huamin Yu[1,3], Tian Cui[1], and Dapeng Xu[1]*

[1]*State Key Laboratory of Superhard Materials, College of physics, Jilin University, Changchun 130000, PR China*
[2]*Changchun Institute of Technology, Changchun 130012, PR China*
[3]*Aviation University Air Force, Changchun 130022, PR China*

(Received 6 January 2019, Received in final form 11 May 2019, Accepted 26 June 2019)

The magnetic properties of Zn_2TiO_4 single crystals were investigated by physical property measurement system (PPMS). The field dependent magnetization (*M-H*) curves showed a weak ferromagnetism at low field and diamagnetism at high field for Zn_2TiO_4 single crystals. The zero-field-cooled (ZFC) and field-cooled (FC) curves further confirmed ferromagnetic behavior of the sample. With the temperature decreasing from 300 to 10 K, the weak ferromagnetism increased slowly. Around 50 K, the M-T curves had a shoulder. After the temperature decreased to 10 K, the ferromagnetism increased significantly. The magnetic mechanism was investigated using the first-principle calculations method. The origin of the ferromagnetic was discussed.

Keywords : Spinel, Zn_2TiO_4 single crystal, Ferromagnetism

1. Introduction

The ZnO–TiO_2 composites have been widely investigated due to their applications in many fields such as paint pigments, gas sensors and catalytic sorbents [1]. The phase diagram of the ZnO–TiO_2 system established by Dulin and Rase [2], indicating that there are three phases: perovskite-type $ZnTiO_3$, spinel-type Zn_2TiO_4 and $Zn_2Ti_3O_8$. The metatitanate $ZnTiO_3$ undergoes decomposition into Zn_2TiO_4 and TiO_2 above 925 ± 25 °C [3]. Yamaguchi *et al.* [4] clarified that $Zn_2Ti_3O_8$ is only a low temperature form of $ZnTiO_3$. There are two types of spinel that are usually observed, the normal and the inverse. Normal spinel compounds generally display the AB_2O_4 stoichiometry with A cations in tetrahedral sites and B cations in octahedral sites [5]. In inverse spinels, B cations are in octahedral sites, while A occupies both octahedral and tetrahedral sites [6]. Zn_2TiO_4 is an inverse spinel, with zinc located at tetrahedral and octahedral sites, while titanium only occupies octahedral sites.

Among the ZnO–TiO_2 composites, the spinel-type Zn_2TiO_4 has attracted great attentions in the field of material sciences. Zn_2TiO_4 is a high-effect regenerable catalytic sorbent for removal of H_2S, As, Se and other contaminants from hot coal gases [7-11]. Due to its excellent dielectric property, Zn_2TiO_4 is also applied in microwave devices [12]. Many studies have been focused on electrical, optical and photoelectrochemical properties to investigate its potential applications [10-14].

Up to now, there was no study about the magnetic properties of Zn_2TiO_4, which makes our work very necessary. As well known, doping impurities and structure defects, including oxygen vacancies, can affect the magnetic behavior of the materials [15-19]. Therefore, we investigate single crystal because of its few defects and impurities which will help in better understanding intrinsic properties of the materials. The high-quality Zn_2TiO_4 crystal was grown by the optical floating zone method. The optical floating zone technique is highly suited to the growth of high purity single crystals, especially metal oxides [20]. Thus, the aim of this work is to investigate the magnetic properties of Zn_2TiO_4 single crystal for the first time for further theoretical studies and practical device fabrications.

2. Experimental and Computational

The high-quality Zn_2TiO_4 single crystal was grown by the optical floating zone method [21]. The powder X-ray diffraction results showed that the as-grown crystal has the spinel-type Zn_2TiO_4 structure. The magnetization as a function of external magnetic field (*M-H*) and magneti-

*Corresponding author: Tel: +86-431-85167955
Fax: +86-431-85167046, e-mail: liuyingbabe@163.com

zation as a function of temperature (*M-T*) at an external magnetic field of 500 Oe were measured at the temperature range from 300 to 3 K using physical property measurement system (PPMS-16). The valence states of elements in sample were determined by X-ray photoelectron spectroscopy (XPS). Furthermore, first principles calculations were also employed to investigate the magnetic property, mainly the spin polarization contributions of the atoms.

3. Results and Discussion

The magnetic properties of Zn_2TiO_4 single crystals are investigated trough PPMS at varied temperature and the magnetization curves (*M-H*) as shown in Fig. 1a. Since using the ground single crystal powder sample, the direction of the external magnetic field does not need to be considered. It can be observed that the sample has ferromagnetic behavior at low field, and the lower the temperature, the larger the area of hysteresis, remanence and coercivity that due to the stronger ferromagnetism (see Fig. 1b). In order to understand the magnetic behavior and magnetic ordering of the sample, the temperature dependence of zero-field-cooled magnetic moment (ZFC) and field-cooled magnetic moment (FC) were measured at an external magnetic field of 500 Oe from 300 to 3 K, as illustrated in Fig. 1c. It is observed that ZFC and FC curves are well bifurcated and the magnetization is always positive, suggesting the ferromagnetic behavior with unblocked ferromagnetic ordering of the sample. With decreasing temperature from 300 to 20 K, the magnetization increased very slowly. However, the FC curve has a shoulder around 50 K. The FC curve at a field of 1000 Oe (also see Fig. 1c) shows the same trend, whereas the position of the shoulder temperature shifts slightly to higher temperature. After the temperature decreased to 20 K, the magnetic moment increased quickly.

As mentioned above, FC curve has a shoulder at 50 K, so the *M-H* curve at 50 K under near $H = 500$ Oe is measured and compared with 30 and 60 K (the inset of Fig. 1c). It can be observed that the magnetization at 50 K is larger than that at 30 and 60 K at an external magnetic field of 500 Oe, which is consistent with what is observed in the FC curve. The results indicate that an anomalous behavior may have appeared at around 50 K, but the change of the magnetization is very small. To further investigate ferromagnetic behavior at temperatures below 20 K, the 10 and 15 K hysteresis loops were later supplemented at low field from −5 to 5 KOe (Fig. 1a). It can be also seen from Fig. 1a that the ferromagnetic curve becomes steeper with the temperature decreasing and the

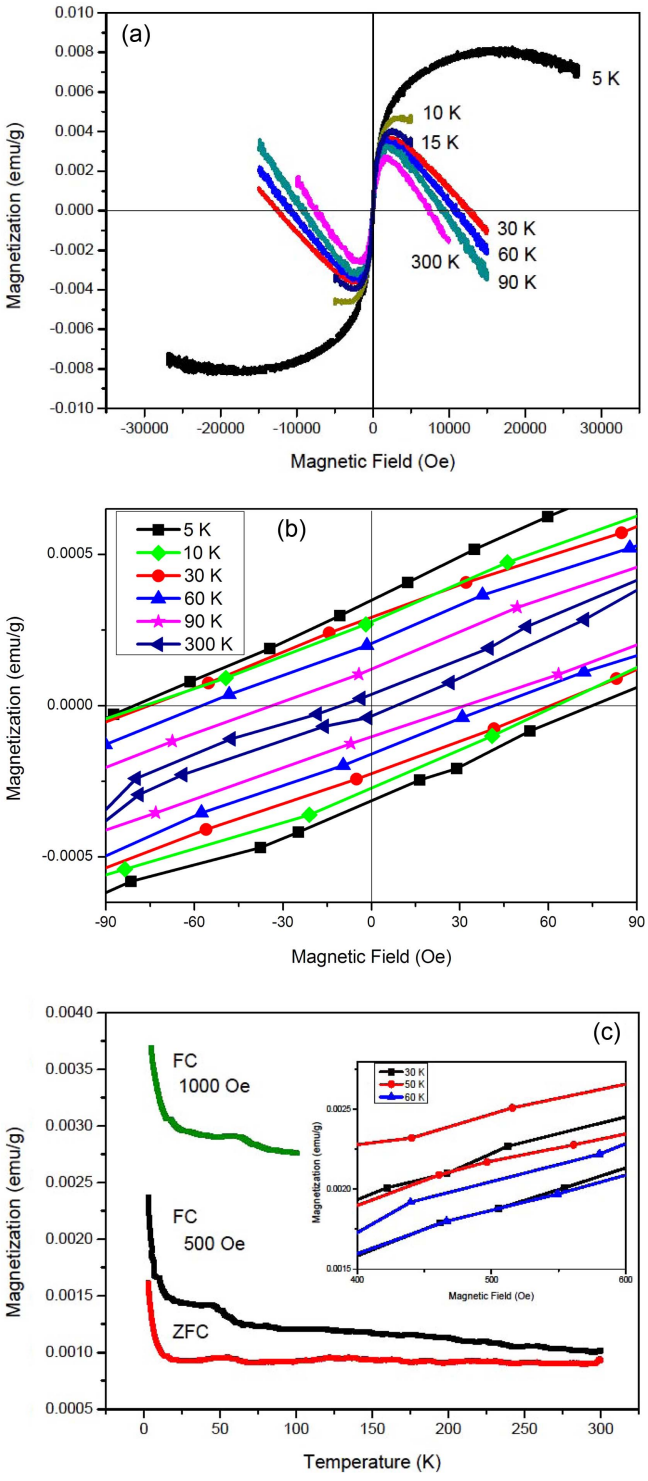

Fig. 1. (Color online) (a) *M-H* curves at different temperatures for Zn_2TiO_4 single crystal powder; (b) a close view of *M-H* curves at 5, 10, 30, 60, 90 and 300 K; (c) Temperature dependent magnetization curves of zero-field-cooled (ZFC) and field-cooled (FC) from 300 to 3 K for Zn_2TiO_4 single crystal powder. The inset shows the magnetization at 30, 50 and 60 K under near H = 500 Oe.

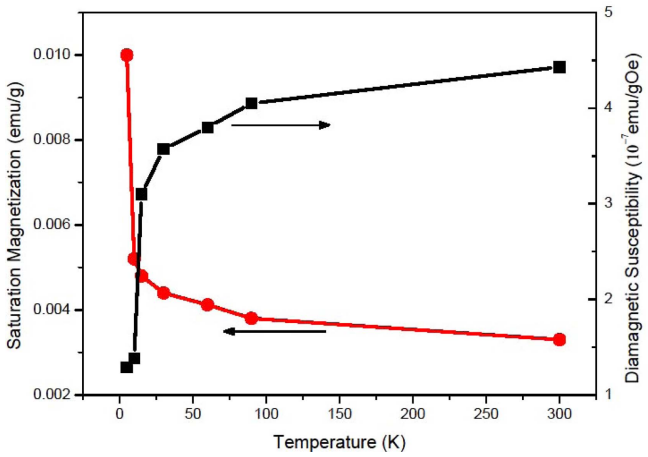

Fig. 2. (Color online) Saturation magnetization and Diamagnetic susceptibility as a function of temperature.

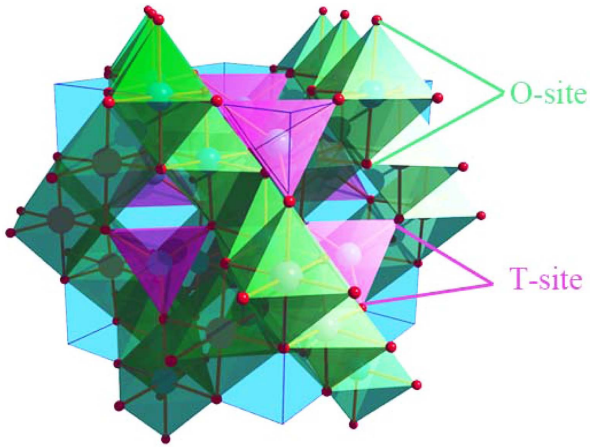

Fig. 3. (Color online) The crystal structure of spinel Zn_2TiO_4.

total magnetization increases obviously when the temperature decreases to 10 K. Fig. 2 exhibits the saturation magnetization (M_s) of ferromagnetism with the temperature, which are obtained from the hysteresis loops. The specific estimation method is described in detail later. As the temperature decreased from 300 to 15 K, the M_s increased very slowly. When the temperature is 5 K, the corresponding M_s increased to 0.01 emu/g quickly. On the other hand, the external magnetic field needed for the sample to reach ferromagnetic saturation gradually increased when the temperature decreased from 300 to 10 K, but they were not more than 4000 Oe. However, when the external magnetic field increased to 17000 Oe, the ferromagnetism reached saturation at 5 K. The *M-H* curves are well corroborated with *M-T* curves. The results show that there is a magnetic orderly shift below 10 K, resulting in a significant enhancement of the ferromagnetism of Zn_2TiO_4 crystals.

Although there are hysteresis loops at the low field, the magnetization of Zn_2TiO_4 single crystals decrease linearly with the increasing of external magnetic field at high field (see Fig. 1a). When the saturation magnetization of ferromagnetism was completely offset by diamagnetic magnetization, the total magnetization became negative as the external magnetic field continued to increase. It can be concluded that *M-H* curves represent the superposition of ferromagnetism and diamagnetism. Since the measurement of magnetism does not require substrates, both ferromagnetism and diamagnetism are intrinsic properties of Zn_2TiO_4. Ferromagnetism is dominant at low field and diamagnetism at high field.

The diamagnetic susceptibility (χ_{dia}) was calculated at high field by the function expressed as:

$$M = M_S - \chi_{dia} \cdot H \quad (1)$$

Where M is the magnetization and H is the external magnetic field. As the magnetization is the superposition of saturation magnetization and diamagnetic moment at high field, the saturation magnetization (M_s) and diamagnetic susceptibility (χ_{dia}) at various temperatures can be obtained by linear fitting of curves of high field. As shown in Fig. 2, the diamagnetic susceptibility is about -4.43×10^{-7} emu/gOe at 300 K and -4.05×10^{-7} emu/gOe at 90 K, which is consistent with the fact that it does not change with temperature. When decreasing the temperature to 10 and 5 K, it decreased to -1.38×10^{-7} and -1.29×10^{-7} emu/gOe rapidly, respectively. It should be the effect of the ferromagnetic enhancement and the increase of M_s in low temperature zone.

The spinel-type Zn_2TiO_4 has a face-centered cubic unit cell, belonging to space group *Fd*-3*m* with $a = 0.84608$ nm and its structure formula can be written as $Zn(TiZn)O_4$. There are 56 atoms in the unit cell, 32 oxygen atoms comprise a face-centered cubic lattice with associated interstitial tetrahedral (T) and octahedral (O) sites (see Fig. 3). The half of divalent Zn cations occupy the T sites, and a stoichiometric mixing of the divalent Zn and tetravalent Ti cations occupy the O sites randomly. The intrinsic diamagnetism is the effect of electron orbital motion induced by external field in Zn_2TiO_4 spinel structure. If there are oxygen vacancies or impurities in the sample, they may result in unoffset electron magnetic moments in the structure, which can produce ferromagnetism by interaction between them. Because our sample is high-quality single crystal, the ferromagnetism at low field of Zn_2TiO_4 is not derived from impurity.

In order to find out the effect of oxygen vacancies on ferromagnetism at low field of Zn_2TiO_4, the single crystal sample was annealed again at 1200 °C in oxygen atmosphere for 20 hours to reduce oxygen vacancies. Sub-

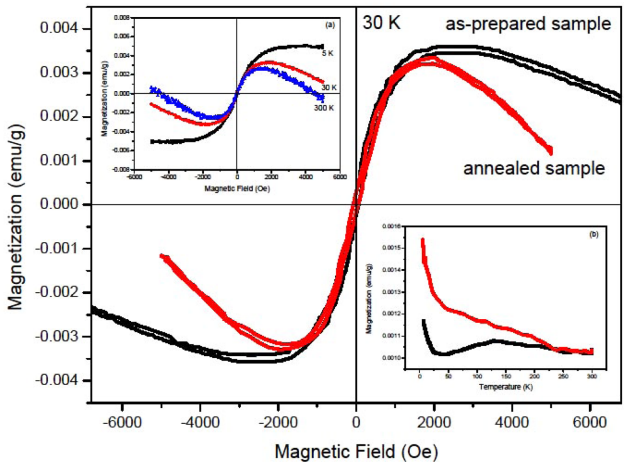

Fig. 4. (Color online) *M-H* curves measured at 30 K for as-prepared and annealed sample in oxygen atmosphere at 1200 °C for 20 hours. Inset (a) *M-H* curves for annealed sample at 300, 30 and 5 K. Inset (b) ZFC and FC curves for annealed sample at $H = 500$ Oe.

sequently, the *M-H* curves (at 300, 30 and 5 K, external magnetic field from −5 to 5 KOe) and ZFC/FC curves (at an external magnetic field of 500 Oe from 300 to 3 K) were measured (Fig. 4). It can be seen that the annealed Zn_2TiO_4 crystal also exhibits ferromagnetic behavior at low field and diamagnetism at high field. By comparison, the hysteresis loops at 300, 30 and 5 K for the as-prepared single crystal sample are steeper than that for the annealed sample. At 30 K, the external magnetic field required for the annealed sample to reach ferromagnetic saturation is 1700 Oe, but 2500 Oe for the as-prepared sample, and the saturation magnetization of the annealed sample is about 0.0043 emu/g, slightly less than that 0.0044 emu/g of the as-prepared sample (shown in Table 1). The comparison of saturation magnetization and coercivity in Table 1 shows that the ferromagnetic weakening caused by annealing sample is very limited, indicating that the oxygen vacancy is only one origin of ferromagnetism of Zn_2TiO_4 single crystal, not all of them.

In addition, we find that the shoulder around 50 K in ZFC and FC curves (Fig. 1c) disappears in annealed sample, as shown in the inset (b) of Fig. 4, which may be related to the oxygen vacancies.

Table 1. Saturation magnetization (M_s) and coercivity (H_c) at 300, 30 and 5 K for as-prepared and annealed sample, respectively.

		300 K	30 K	5 K
as-prepared sample	M_s (emu/g)	0.0033	0.0044	0.01
	H_c (Oe)	8.643	61.446	80.902
annealed sample	M_s (emu/g)	0.0032	0.0043	0.006
	H_c (Oe)	7.962	58.87	68.545

From the element composition of Zn_2TiO_4, the electron magnetic moment may come from Ti^{3+} ion. The ideal valence state of Ti is +4 in the Zn_2TiO_4 spinel structure because of the octahedron ion formed by the random occupation of Zn and Ti. But even the single crystal sample, the internal ion vacancies will also exist. If there are Ti^{3+} ions from Ti-site cation vacancies in single crystal sample, the randomly occupied Ti^{3+} ions may produce ferromagnetism by Ti^{3+}-Ti^{3+} super-exchange interaction.

To have a deep look into the mechanism of magnetic properties of Zn_2TiO_4, a first principles calculation is handled via CASTEP MODULE of Materials Studio. A primitive cell is employed which is derived from ICSD: 080851. Although the computational unit is described as Zn_2TiO_4, it actually can be considered as intrinsic defected crystal due to the fractional occupation of zinc and titanium.

Perdew Berke Ernzerhof (PBE) functional within the generalized gradient approximation [22] is applied accompany with norm-conserving potential, and the cutoff energy is 830 eV in self-consistent total energy minimization with initial spin 3 μ_B per atom. The spin density of states, which is the most important function for the explanations of the magnetism phenomena, is shown in Fig. 5 (total) and Fig. 6 (projections to atom).

It is clear to find that the material is ferromagnetic proved by the net spin of about 7 electrons per cell (primitive). The magnetic moment is mainly contributed by d-state electrons, while p-state electrons offer the next, and s-state electrons give almost null. Note that p-state electrons contribute negative at just below the Fermi Level.

The projective Partial Density of States (PDOS) of

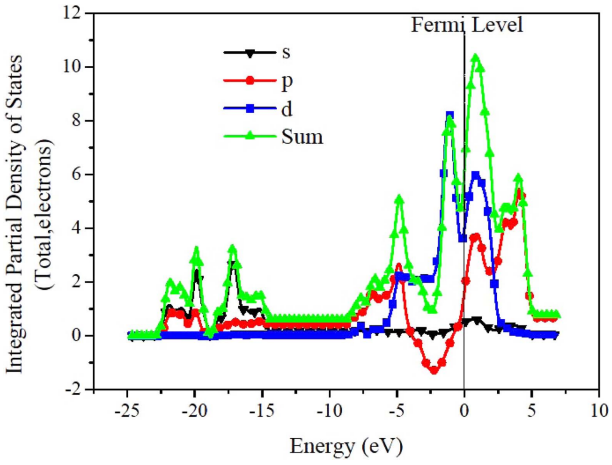

Fig. 5. (Color online) The total Partial Density of States.

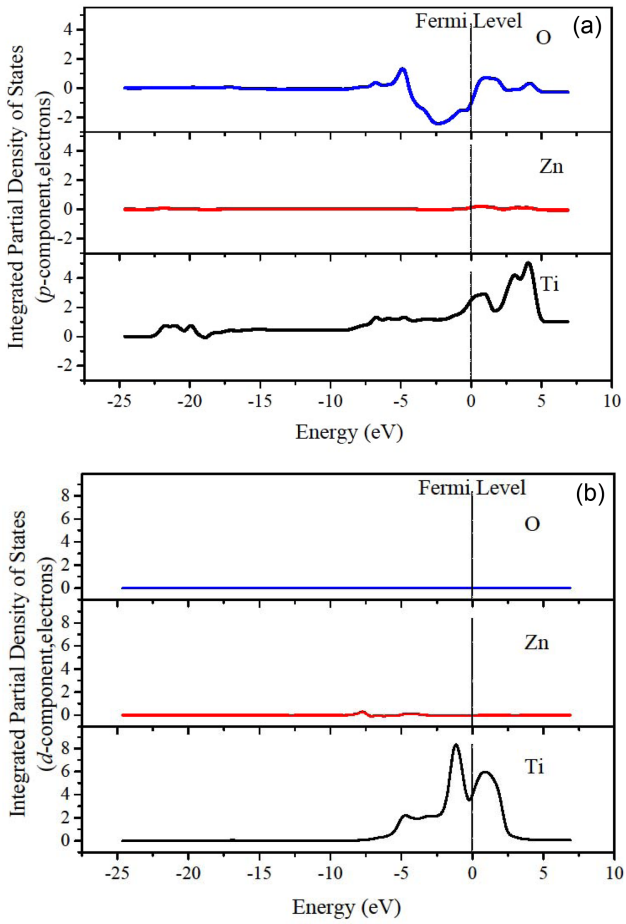

Fig. 6. (Color online) The Partial Density of States project of atomic orbitals (a) p-component; (b) d-component.

different atoms is show in Fig. 6, where the s-states are omitted due to their minor contribution to the total spin density of states. As shown in Fig. 6, for the p-states, Titanium contributes the most, and its decrease in Fig. 5 is definitely from Oxygen atoms. For d-states, only Titanium plays the role in magnetic moment.

In summarize, the ferromagnetic properties of Zn_2TiO_4 come from the p- and d-states of Titanium, and Zinc has little contributions while Oxygen plays the negative role.

For investigating the electronic state of Titanium, X-ray photoelectron spectroscopy (XPS) measurement was performed for Zn_2TiO_4 single crystal, as shown in Fig. 7. The binding energy of Ti-2*p* can be divided into four bonds at 457.75, 458.77, 463.77 and 464.95 eV which represent Ti^{3+}-$2p_{3/2}$, Ti^{4+}-$2p_{3/2}$, Ti^{3+}-$2p_{1/2}$ and Ti^{4+}-$2p_{1/2}$, respectively [23, 24]. It indicates the existence of Ti^{3+} ions in the sample which may be a source of ferromagnetism of the sample.

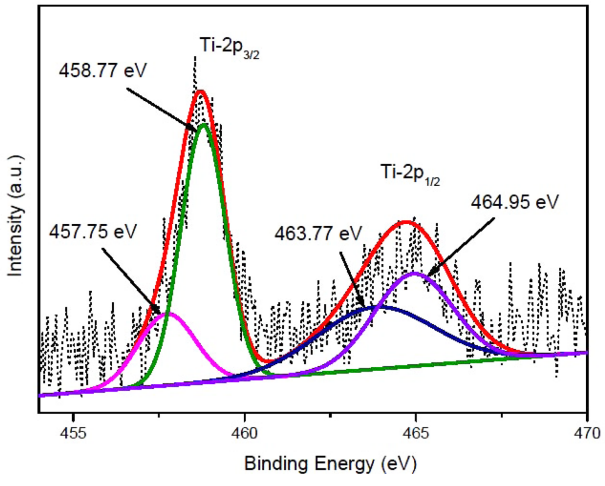

Fig. 7. (Color online) Ti-2*p* XPS of Zn_2TiO_4 single crystal.

4. Conclusion

In conclusion, the Zn_2TiO_4 single crystals show ferromagnetism and diamagnetism at different field. Ferromagnetism is dominant at low field and diamagnetism at high field. With the temperature decreasing from 300 to 10 K, the weak ferromagnetism increased slowly. Around 50 K, the *M-T* curves have a shoulder, indicating an anomalous behavior. After the temperature decreased to 10 K, the ferromagnetism increased significantly, showing that the ferromagnetic mutation occurred below 10 K. The effects of Ti^{3+} ions and oxygen vacancies on the ferromagnetism of the Zn_2TiO_4 single crystals were also discussed.

Acknowledgements

The financial support from the National Foundation for Fostering Talents of basic Science (Grant No. J1103202), the National Natural Science Foundation of China (Grant No. 11274137, 11074090, 11304113), the Education and research project of Jilin Province education department (No. 2016401) and the Open Project of State Key Laboratory of Inorganic Synthesis and Preparative Chemistry (Jilin University) (No. 2017-6) are greatly appreciated.

References

[1] T. Akilan, N. Srinivasan, and R. Saravanan, Materials Science in Semiconductor Processing **30**, 381 (2015).
[2] F. H. Dulin and D. E. Rase, J. Am. Ceram. Soc. **43** (1960).
[3] Alima Mebrek, Safia Alleg, Sihem Benayache, and Mohamed Benabdeslem, Ceramics International **44**, 10921 (2018).
[4] O. Yamaguchi, M. Morimi, H. Kawabata, and K. Shimizu, J. Am. Ceram. Soc. **70** (1987).
[5] Hk Müller-Buschbaum, J. Alloy Compd. **349**, 49 (2003).
[6] E. R. Leite, J. A. Varela, E. Longo, and C. A. Paskoci-

mas, Ceram Int. **21**, 153 (1995).
[7] Y. Yang, X. W. Sun, B. K. Tay, J. X. Wang, Z. L. Dong, and H. M. Fan, Adv. Mater. **19**, 1839 (2007).
[8] L. Alonso, J. M. Palacios, and R. Moliner, Energy & Fuels. **15**, 1396 (2001).
[9] K. Jothimurugesan and S. K. Gangwal, Ind. Eng. Chem. Res. **37**, 1929 (1998).
[10] Z. W. Wang, S. K. Saxena, and C. S. Zha, Phys. Rev. B **66**, 0241031 (2002).
[11] Y. Yang, R. Scholz, H. J. Fan, D. Hesse, U. Gosele, and M. Zacharias, Acs Nano **3**, 555 (2009).
[12] Liang Li, Fangfei Li, Tian Cui, Qiang Zhou, and Dapeng Xu, Phys. Status Solidi A **209**, 2596 (2012).
[13] A. C. Chaves, S. J. G. Lima, R. C. M. U. Araújo, M. A. M. A. Maurera, E. Longo, P. S. Pizani, L. G. P. Simões, L. E. B. Soledade, A. G. Souza, and I. M. G. dos Santos, J. Solid State Chem. **179**, 985 (2006).
[14] M. V. Nikolić, N. Obradović, K. M. Paraskevopoulos, T. T. Zorba, S. M. Savić, and M. M. Ristić, J. Mater. Sci. **43**, 5564 (2008).
[15] Dongyoo Kim, Jisang Hong, Young Ran Park, and Kwang Joo Kim, J. Phys.: Condens. Matter **21**, 195405 (2009).
[16] Menglei Li, Jia Li, Long-Qing Chen, Gu Bing-Lin, and Wenhui Duan, Phys. Rev. B **92**, 115435 (2015).
[17] G. S. Chang, J. Forrest, E. Kurmaev, A. N. Morozovska, M. D. Glinchuk, J. A. McLeod, A. Moewes, T. P. Surkova, and Nguyen Hoa Hong, Phys. Rev. B **85**, 165319 (2012).
[18] Peng Zhan, Weipeng Wang, Can Liu, Yang Hu, Zhengcao Li, Zhengjun Zhang, PengZhang, Baoy Wang, and Xingzhong Cao, J. Appl. Phys. **111**, 033501 (2012).
[19] R. Murugan, G. Vijayaprasath, T. Mahalingam, and G. Ravi, Ceramics International **42**, 11724 (2016).
[20] H. Dabkowska, A. Dabkowski, P. Rudolph (Ed.), Hand book of Crystal Growth, Elsevier (2015) pp 281-329.
[21] L. Li, H. Yang, D. J. Wang, G. L. Feng, B. X. Li, Z. M. Gao, D. P. Xu, Z. H. Ding, and X. Y. Liu, J. Cryst. Growth. **312**, 3561 (2010).
[22] J. P. Perdew, K. Burke, and M. Ernzerhof, Phys. Rev. Lett. **77**, 3865 (1996).
[23] C. Malitesta, I. Losito, F. Scordari, and E. Schingaro, Eur. J. Mineral **7**, 847 (1995).
[24] L. Li, S. H. Gao, T. Cui, B. X. Li, Q. Zhou, H. M. Yuan, and D. P. Xu, RSC. Adv. **7**, 35477 (2017).